Risk adaptive planning with biology-based constraints may lead to higher tumor control probability in tumors of the canine brain: A planning study

Radonic, Stephan ; Schneider, Uwe ; Besserer, Jürgen ; Meier, Valeria S ; Rohrer Bley, Carla

DOI: https://doi.org/10.1016/j.ejmp.2024.103317

Physica Medica 119 (2024) 103317

Contents lists available at ScienceDirect

Physica Medica

journal homepage: www.elsevier.com/locate/ejmp

Original paper

Risk adaptive planning with biology-based constraints may lead to higher tumor control probability in tumors of the canine brain: A planning study

Stephan Radonic [a,b,*], Uwe Schneider [a,c], Jürgen Besserer [a,c], Valeria S. Meier [a,b], Carla Rohrer Bley [b]

[a] Department of Physics, University of Zurich, Zurich, Switzerland
[b] Division of Radiation Oncology, Small Animal Department, Vetsuisse Faculty, University of Zurich, Zurich, Switzerland
[c] Radiotherapie Hirslanden AG, Rain 34, Aarau, Switzerland

ARTICLE INFO

Keywords:
Risk-adaptive optimization
Biologic objective function
TCP
NTCP
Biology-based
IMRT
Intensity-modulated radiation therapy
Dog
Brain tumor
Radiation therapy

ABSTRACT

Background: Classical radiation protocols are guided by physical dose delivered homogeneously over the target. Protocols are chosen to keep normal tissue complication probability (NTCP) at an acceptable level. Organs at risk (OAR) adjacent to the target volume could lead to underdosage of the tumor and a decrease of tumor control probability (TCP). The intent of our study was to explore a biology-based dose escalation: by keeping NTCP for OAR constant, radiation dose was to be maximized, allowing to result in heterogeneous dose distributions.

Methods: We used computed tomography datasets of 25 dogs with brain tumors, previously treated with 10x4 Gy (40 Gy to PTV D_{50}). We generated 3 plans for each patient: A) original treatment plan with homogeneous dose distribution, B) heterogeneous dose distribution with strict adherence to the same NTCPs as in A), and C) heterogeneous dose distribution with adherence to NTCP < 5%. For plan comparison, TCPs and TCP equivalent doses (homogenous target dose which results in the same TCP) were calculated. To enable the use of the generalized equivalent uniform dose (gEUD) metric of the tumor target in plan optimization, the calculated TCP values were used to obtain the volume effect parameter a.

Results: As intended, NTCPs for all OARs did not differ from plan A) to B). In plan C), however, NTCPs were significantly higher for brain (mean 2.5% (SD±1.9, 95%CI: 1.7,3.3), $p < 0.001$), optic chiasm (mean 2.0% (SD±2.2, 95%CI: 1.0,2.8), $p = 0.010$) compared to plan A), but no significant increase was found for the brainstem. For 24 of 25 of the evaluated patients, the heterogenous plans B) and C) led to an increase in target dose and projected increase in TCP compared to the homogenous plan A). Furthermore, the distribution of the projected individual TCP values as a function of the dose was found to be in good agreement with the population TCP model.

Conclusion: Our study is a first step towards risk-adaptive radiation dose optimization. This strategy utilizes a biologic objective function based on TCP and NTCP instead of an objective function based on physical dose constraints.

1. Background

Classical radiation protocols are guided by physical dose, delivered homogeneously over the target. Such fixed radiation protocols provide a safe measure for a treated population, as the risk for complications can be set to an acceptable level. Due to the individual patient's tumor size and location, however, fixed protocols might relatively underdose certain patients: if tumors are smaller or not close to organs at risk, radiation dose could safely be escalated for this individual patient. Escalated radiation dose levels will then potentially lead to better tumor control [1,2]. In general, dose can be escalated homogeneously throughout the whole or parts of the target, where different dose levels are prescribed to "boost" regions containing most tumor cells [3–5]. Alternatively, intensity-modulated radiation therapy (IMRT) can "paint" higher doses to more radio-resistant biologic targets such as hypoxic areas, identified in functional imaging such as positron emission tomography (PET) [6–8]. Both selective boosting techniques can lead to substantial increases in tumor control probability (TCP), if subvolumes up to 60%–80% receive a modest 20%–30% additional dose above the minimal peripheral (prescribed) dose [9,10]. Tome et al. [10] calculated TCP increases with both, increasing boost dose ratio and boosted

* Corresponding author.
E-mail address: stephan.radonic@uzh.ch (S. Radonic).

https://doi.org/10.1016/j.ejmp.2024.103317
Received 3 July 2023; Received in revised form 27 November 2023; Accepted 6 February 2024
Available online 1 March 2024

volumes, finding a saturation/plateau (=maximum increase in TCP) after boost dose ratios of 1.2–1.3. Only if the very highest proportions of the tumor volumes could be boosted (>90%–95%), the plateau was again overcome, and an additional gain in TCP was seen [10]. A 15% dose increase (1.15 ratio boost of dose) to 60%–80% of the volumes, achieved an increase of 6%–11% in TCP [10]. Apart from the technical complexity of dose-painting, the tumor-biologic fluctuations during a patient's treatment make this approach highly complex [11,12]. Such a complex individualistic approach remains a long-term objective of collaborative effort in current radiation research. Another way to exploit advanced radiation therapy delivery tools could be to use the expected risk for radiation toxicity (late complications). A patient's accepted risk of late complications is usually set below 5% [13–15]. These 5%, however, are often not exhausted in classical radiation plans with homogeneous physical dose distribution, therefore in many patients the risk is much lower. Assigning a fixed risk of toxicity would lead to the chance to exploit the patient's highest accepted dose, and potentially increase the individual and the population's tumor control. We want to explore such a "biology-based" dose escalation: by holding the normal tissue complication probability (NTCP) for organs at risk constant, we want to maximize the radiation dose in all regions possible. While this idea is not a novelty [16–18], it is not commonly used. We aim for treatment plans with the highest amount of tumor control, allowing heterogeneous dose distribution. Tumor dose will be limited by the expected toxicity, using biological response models (TCP/NTCP) during treatment planning. These models help to understand the potential consequences of such a heterogeneous dose on tumor control, as an addition to the physical quantities of absorbed dose and volume [19–25]. Surprisingly, model predictions deflect the "conventional wisdom" that the minimum tumor dose is the major determinant of tumor control: a modest underdosage in a partial volume might not reduce TCP if the dose can be compensated in another region [10,26,27]. In order to compare the effects of non-uniform dose distributions, a metric for characterizing these distributions is needed. The equivalent uniform dose (EUD) provides such a possible metric. The first applications of the biology-based generalized EUD (gEUD) in treatment planning were considered useful, improving the sparing of organs at risk while maintaining the coverage of the target dose [28–30]. As an additional advantage, the gEUD considers tissue-specific characteristics during the planning process, which cannot be done with the simple dose-volume-based optimization [28]. Similar approaches for EUD versus regular planning objectives (albeit with strong dose homogeneity requirements) have been made before and consistently show that regular plans, based on dose-volume-based objective functions, have generally higher amount of doses in the organs at risk [30]. This is because in dose-volume-based objectives, the optimization process will stop, once the goals are met, while the gEUD based optimization process has the advantage to continue until the best solution is found.

Herein, we investigated a possible advantage of deliberate heterogeneous radiation dose delivery on tumor control. We used the concepts of gEUD and tested the possibility for future clinical application. For this planning study, we used datasets from our dog patients with brain tumors and generated 3 plans for each patient: (A) (classical) homogeneous dose distribution within the planning target volume (PTV), (B) heterogeneous dose distribution with concurrent strict adherence to the same NTCPs as in (A), and (C) heterogeneous dose distribution with adherence to a prior defined NTCP in the organs at risk, as deemed clinically acceptable for a prospective clinical study. We used prior derived gEUD values as planning constraints [31]. As a readout, TCP and NTCPs were compared between the three groups.

2. Methods

2.1. Study aim and design, patient and tumor characteristics

We aimed to investigate a possible advantage of deliberate heterogeneous radiation dose delivery on tumor control. For this, we used a theoretical planning approach and included pre-existing datasets from dogs with magnetic resonance imaging (MRI) or computed tomography (CT) imaging confirmed meningioma. These brain tumor patients were treated with radiation therapy at the Division of Radiation Oncology of the Vetsuisse Faculty, University of Zurich between September 2017 and March 2020. The target volumes and organs at risk (OAR) were contoured in a facility internal standardized manner as previously published by our research group [32]. In brief, the gross tumor volume (GTV) was delineated on co-registered contrast-enhanced CT or MR images. The margins for the clinical target volume (CTV), accounting for subclinical microscopic disease extension, was defined to be 2 mm for meningeal and pituitary tumors and 3–5 mm for glial tumors, respecting anatomical boundaries such as bone. The CTV margin then was extended 3-dimensionally by 2 mm to define the PTV, accounting for setup uncertainties in daily image-guided photon treatment. The PTV margin had been established earlier with the prior described individually fitted positioning device, consisting of a bite block and a vacuum cushion (BlueBag BodyFix, Elekta AB, Stockholm, Sweden). Further, brain, brainstem and GTV/brain ratio were documented.

2.2. Treatment planning

Treatment was planned as deliverable with volumetric modulated arc therapy (VMAT)/ RapidARC. Each dataset was planned with three plans (Table 1). D2%, D50% and D98% is the dose to 2%, 50% and 98% of the volume.

(A) Plan 1_hom: homogeneous dose distribution within the PTV, with a prescription of 10 × 4 Gy (40 Gy to PTV D_{50}) [32,33]. For the homogeneous plans (Plan 1_hom), the dose was prescribed to $D_{50\%}$, and $D_{98\%}(= D_{near-min})$ and $D_{2\%}(= D_{near-max})$ was reported [34,35]. For adequate PTV coverage, also $D98/95$ had to be fulfilled: 98% of the target volume had to be covered by 95% of the prescribed dose (i.e. 98% of PTV receives ≥ 38 Gy), in order to achieve a steep DVH.

(B) Plan 2_het1: heterogeneous dose distribution with 10 fractions and concurrent strict adherence to the same NTCPs as in (1). For the heterogeneous plans with concurrent strict adherence to the same NTCPs as in plan A (Plan 1_hom), only $D_{98\%}$ was fixed, in addition to the NTCP adherence. PTV coverage was limited only in the upper dose, for patient safety reasons - $D_{2\%}$ was fixed at $D2/130$ (i.e. max 2% of PTV received ≥ 52 Gy). $D_{50\%}$ could be as high as possible, as long as NTCP adherence was met.

(C) Plan 3_het2: heterogeneous dose distribution with 10 fractions and adherence to a prior defined NTCP in the organs at risk, as deemed clinically acceptable for a prospective clinical study. For the heterogeneous plans with adherence to the defined NTCPs (of 5%) (Plan3_het2), only $D_{2\%}$ was fixed at D2/130 (i.e. max 2% of PTV receives ≥ 52Gy). Again, $D_{50\%}$ could be as high as possible, as long as the NTCP adherence of 5% was met. Hence, for these plans, no uniform prescription was applicable.

We planned with the treatment planning software Eclipse™ Planning system version 15.3, including Photon Optimizer (PO) with fine settings (1.25 mm) (Varian Medical Systems, Palo Alto, CA). We used the same VMAT specifications for all plans and calculated with AAA 15.1.51 and a fine grid of 1.25 mm. For the first plan variant (Plan 1_hom), OAR absorbed dose was minimized at the planning radiation oncologist's discretion, as done in clinical routine. The actual dose corresponding to the calculated gEUD (gEUD is formally explained in Section 2.7) was then inserted as a constraint in the optimization (Plan 2_het1). Plan 2_het 1 was normalized to correspond the first plan (Plan 1_hom) in the respective NTCPs of the organs at risk. For control purposes the NTCP-values were extracted from both plans [36,37].

2.3. Biology-based constraints for optimization

For the third plan variant, gEUD values corresponding to NTCP of 5% for the respective OARs were extracted; we took parameter sets from Burman et al. (a = 6.25, m = 0.14, TD50 = 65 Gy for brainstem, a = 4, m = 0.15, TD50 = 60 for brain, and the optic chiasm a = 4, m = 0.14, TD50 = 65 Gy): alpha/beta value = 2 Gy, which are based on fits to human normal tissue data compiled by Emami et al. as previously described. The gEUDs were plotted against NTCP from a 30 × 2 Gy protocol used for human glioma irradiation [24,31,38]. In order to adjust for fraction size and fraction number in the new 10-fraction protocol, the parameter gEUD was then converted to a biologically equivalent gEUD using the linear-quadratic (LQ) model. The biologically equivalent gEUD for NTCP 5% for brainstem and brain was used as an upper limit (upper gEUD) during plan optimization.

Hence, in Plan 1_hom, dose prescription follows the published guidelines [34,35]. For the deliberately heterogeneous planned plans, we move away from classical prescription: the conditions now only include a fixed (either same-risk or at 5%) NTCP. Furthermore, the upper constraint of *D2/130* of the original prescription was the upper limit for future patients' safety.

2.4. Obtaining model parameters

In [39], a novel analytical population TCP model was derived. The model was fitted to clinical survival data of dog patients [33,40,41] undergoing radiation therapy for a brain tumor. Through this procedure, model parameters were obtained which enabled the calculation of TCP. In [39,42], the population TCP model was derived by analytically incorporating variations of tumor volume sizes. As in [42], it was assumed that the underlying frequency distribution of the present tumor volume sizes in the population is exponentially distributed. However, it was conjectured that there is a minimal tumor volume below which tumors are unlikely to be clinically observed [39,42]. Thus the frequency distribution is given by

$$f^{obs}_{V_{avg},V_C}(V) = \frac{V_{avg}+V_C}{V^2_{avg}}\left(1-\exp\left(-\frac{V}{V_C}\right)\right)\exp\left(-\frac{V}{V_{avg}}\right) \tag{1}$$

which results in modifying the exponential distribution by a detection rate $1-\exp\left(-\frac{V}{V_C}\right)$, where V_{avg} is the average volume of tumors in a patient population and V_C is a surrogate measure which describes the limited clinical observability of small tumor volumes [39]. The population TCP is then given by [39]

$$\int_0^\infty \frac{(V_{\text{avg}}+V_C)}{V^2_{\text{avg}}}\exp\left(-\frac{V}{V_{\text{avg}}}\right)\left(1-\exp\left(-\frac{V}{V_C}\right)\right)\exp(-\rho S V)\,dV \tag{2}$$

$$= \frac{V_{\text{avg}}+V_C}{(\rho S V_{\text{avg}}+1)(\rho S V_{\text{avg}} V_C + V_{\text{avg}} + V_C)} \tag{3}$$

where S is the survival model function, which for the LQ model is given by $S(D,d_f,\alpha,\beta) = e^{-\alpha D-\beta d_f D}\,e^{\gamma T}$. T is the overall treatment time and $\gamma = \frac{\log(2)}{T_D}$ with T_D being the tumor doubling time [43,44]. For fitting the model to clinical data, as in [39] $\frac{\alpha}{\beta}$ was constrained to $\frac{\alpha}{\beta} = 8$ Gy, $V_{\text{avg}} = 3.37\ \text{cm}^3$ and $V_C = 1.6\ \text{cm}^3$ as determined from the clinical data.

In order to determine the errors of the obtained parameters, we used the bootstrapping method [45]. From the dataset of clinical data D we randomly select observations d_i with replacement to create bootstrapping samples $S_n = \{d_i,\dots\}$. A particular data point d_i can occur multiple times in a bootstrapping sample S_n. For each sample S_n the fitting procedure is performed and yields a set of fitting parameters with the corresponding χ^2: $p_n = \{\alpha, a, T_D\}_n$. From the sets of fitting parameters $\{p_1,\dots,p_N\}$ a frequency distribution can be calculated for each fitting parameter as well as for χ^2. From the frequency distributions we can obtain the 95% intervals and other statistics.

2.5. Estimation of tumor control probability

The TCP as modeled by Nahum and Tait [46] is given by

$$TCP = e^{-N_S} \tag{4}$$

where N_S is the number of surviving clonogenic cells. Webb and Nahum [47] derived a model for the TCP with non-uniform clonogenic cell density and non-uniform dose.

For each voxel of the CTV, the absorbed dose for the respective fraction is recorded. The recorded dose values are used to calculate the cell survival of the particular CTV voxel. The cell survival at fraction f of a voxel i is given by

$$S_i^f = S(D_i^f,\alpha,\beta) \tag{5}$$

where S is the survival model function and D_i^f is the dose [Gy] which the voxel i is exposed to at fraction f. In case of the LQ Model [48] the cell survival function is given by

$$S(D_i^f,\alpha,\beta) = e^{-\alpha D_i^f-\beta(D_i^f)^2} \tag{6}$$

In [43], the LQ-model is combined with an assumed tumor repopulation factor. Furthermore, in [49], the dependence of the survival rate on the elapsed time is characterized by an exponential decrease. The cell survival in voxel i after M fractions is

$$S_i = \prod_{f=0}^{M} S_i^f \tag{7}$$

The patient survival (TCP) after a follow-up period τ is then given by

$$TCP = \prod_{i=0}^{N} e^{-\rho_i V_i S_i e^{\gamma T} e^{a\tau}} \tag{8}$$

where V_i is the volume and ρ_i is the cell density at voxel i. Here, a homogenous ($\forall i : \rho_i = \rho$) cell density $\rho = 10^7$ cells/cm^3 was assumed inside the CTV. $e^{\gamma T}$ accounts for the effective tumor-cell repopulation rate, where $\gamma = \ln(2)/T_D$, T_D being the tumor doubling time and T being the treatment time. For the treatment time T in days, seven-fifth times the number of fractions M was used if $M > 5$, else it was assumed to be equal to the number of fractions. $e^{a\tau}$ characterizes exponential dependence of the survival rate on the elapsed time. The TCPs were calculated for a follow-up time of 3 years.

In a Monte Carlo procedure we sampled the calculation parameters $p_i = \alpha, a, T_{D_i}$ from the distribution $\{p_1,\dots,p_N\}$ obtained by bootstrapping in Section 2.4 and used them to calculate a TCP distribution. From the TCP distribution we can obtain the error margins. This was done by calculating the 15.87 and 84.13 percentiles of the distribution, which correspond to $\pm 1\sigma$.

2.6. TCP equivalent dose

It is common practice to plot and evaluate the TCP against the prescribed dose. In classical RT where the dose distribution inside the clinical target volume (CTV) is more or less homogenous, this is an appropriate procedure. However, this is not suitable for an inhomogeneous dose distribution. As the TCP is a product of the TCPs of individual voxels, also the mean dose is not a viable measure for comparing different inhomogeneous plans. Thus, here we introduced the concept of the TCP equivalent dose. The TCP equivalent dose of an RT plan with inhomogeneous dose distribution within the CTV, is equal to the dose of a perfectly homogeneous RT plan which would yield the same TCP.

$$TCP_{hom} \overset{!}{=} TCP_{het} \tag{9}$$

$$e^{-\rho V e^{-D_{\text{hom}}\left(\alpha+\beta d_{hom}-\frac{7}{5}\frac{\gamma}{d_{hom}}\right)+a\tau}} = \prod_{i=0}^{N} e^{-\rho_i V_i e^{-D_i(\alpha+\beta * d_i-\frac{7}{5}\frac{\gamma}{d_i})+a\tau}} \tag{10}$$

$$e^{-\rho V e^{-D_{\text{hom}}\left(\alpha+\beta d_{hom}-\frac{7}{5}\frac{\gamma}{d_{hom}}\right)+a\tau}} = e^{\left(-\sum_{i=0}^{N}\rho_i V_i e^{\left(-D_i(\alpha+\beta*d_i-\frac{7}{5}\frac{\gamma}{d_i})+a\tau\right)}\right)} \tag{11}$$

We assume that all N voxels are of equal size $V_i = \frac{V}{N}$ and that the cell density $\forall i : \rho_i = \rho$ is homogeneous. Thus

$$e^{-\rho V e^{-D_{\text{hom}}\left(\alpha+\beta d_{hom}-\frac{7}{5}\frac{\gamma}{d_{hom}}\right)+a\tau}} = e^{\left(-\rho V_i\sum_{i=0}^{N} e^{\left(-D_i(\alpha+\beta*d_i-\frac{7}{5}\frac{\gamma}{d_i})+a\tau\right)}\right)} \tag{12}$$

logarithm on both sides yields

$$-\rho V e^{-D_{\text{hom}}\left(\alpha+\beta d_{hom}-\frac{7}{5}\frac{\gamma}{d_{hom}}\right)+a\tau} = -\rho V_i\sum_{i=0}^{N} e^{\left(-D_i(\alpha+\beta*d_i-\frac{7}{5}\frac{\gamma}{d_i})+a\tau\right)} \tag{13}$$

$$-D_{\text{hom}}\left(\alpha+\beta d_{hom}-\frac{7}{5}\frac{\gamma}{d_{hom}}\right)+a\tau = \log\left(\frac{V_i}{V}\sum_{i=0}^{N} e^{\left(-D_i(\alpha+\beta*d_i-\frac{7}{5}\frac{\gamma}{d_i})+a\tau\right)}\right) \tag{14}$$

which finally leads to

$$D_{\text{hom}} = \frac{\log\left(\frac{1}{N}\sum_{i=0}^{N} e^{\left(-D_i(\alpha+\beta*d_i-\frac{7}{5}\frac{\gamma}{d_i})+a\tau\right)}\right)-a\tau}{-(\alpha+\beta d_{hom}-\frac{7}{5}\frac{\gamma}{d_{hom}})} \tag{15}$$

For the calculations we used parameters from Table 1. For all patients the prescribed fractionation in the homogeneous plan was a 10 × 4.0 Gy scheme (40 Gy to PTV D_{50}), thus $d_{hom} = 4.0$ Gy. It shall be noted that the resulting number of fractions when applying D_{hom} from Eq. (15) in fractions of $d_{hom} = 4.0$ Gy, can differ from the 10 fractions used in the original homogeneous dose plan.

2.7. Generalized equivalent uniform dose

Ideally, we could use the previously established TCP and TCP equivalent dose variables directly for RT planning. As it is our goal to create RT plans with deliberate inhomogeneous dose distributions, with which real canine patients can be treated, the RT planning has to be done using the commercial Varian Eclipse TPS used at our facility. The aforementioned TCP and TCP equivalent dose variables are not available to us in Varian Eclipse for use during treatment plan optimization. However, Varian Eclipse enables using the generalized equivalent uniform dose (gEUD) as an optimization objective for treatment planning. Particularly for treatment planning with deliberate heterogeneous dose distributions, the gEUD is a useful tool. For tumors, the equivalent uniform dose (EUD) is defined as the biologically equivalent uniform dose which would match the cell kill in the tumor volume of the actual nonuniform dose distribution.

$$gEUD = \left(\frac{1}{N}\sum_{i=1}^{N}(D_i)^a\right)^{\frac{1}{a}} \tag{16}$$

where N is the number of voxels in the tumor, D_i is the dose in the voxel i and a is a tumor specific parameter which is a model for the dose-volume effect. To determine a we used the orthogonal least squares methods. In a first step for all N_p patients the gEUD values $(gEUD_k)_a$ were computed for a values in the interval $[-100.0, -0.2]$ with step size 0.2. Also the TCP_k values were calculated as described in Section 2.5. Next, as illustrated in Fig. 1, the orthogonal distance $(\Delta_{\perp_k})_a$ was obtained. The angle Ω was calculated using the derivative of the population TCP function (Eq. (3))

$$\Omega = \arctan\left(\frac{\partial(TCP_{pop})}{\partial D}\Big|_{D=(gEUD_k)_a}\right) \tag{17}$$

also

$$\cos(\Omega) = \frac{(\Delta_{\perp_k})_a}{\Delta(TCP_k)_a} \tag{18}$$

where

$$\Delta(TCP_k)_a = |TCP_{pop}((gEUD_k)_a) - TCP_k| \tag{19}$$

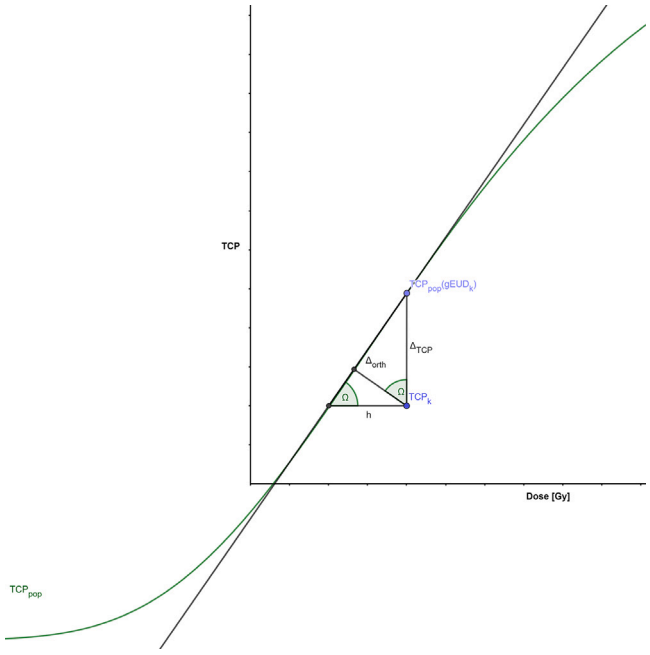

Fig. 1. Illustration of the orthogonal least squares fitting.

with that $(\Delta_{\perp_k})_a$ is given by

$$(\Delta_{\perp_k})_a = \cos(\Omega)\Delta(TCP_k)_a \tag{20}$$

For each value of a the sum of the orthogonal distances was computed

$$\chi_a^2 = \sum_{k=1}^{N_p}(\Delta_{\perp_k})_a \tag{21}$$

We then found the a_{opt} value for which the sum of the orthogonal distances is smallest

$$a_{opt} = \underset{a\in[-100.0,-0.2]}{\text{argmin}}\ \{\chi_a^2\} \tag{22}$$

The TCP values for the heterogeneous plans variant 1 and 2 were analyzed in two ways. First, by fitting all data points from every RT plan of all patients together, producing a single a_{opt} value. Second, by grouping patients into three classes based on tumor volume and fitting each category separately, resulting in three distinct a_{opt} values.

2.8. Plan comparison

Normal tissue complication probability (NTCP) of brain, brainstem and optic chiasm was computed as previously described and documented for each of the three different treatment plans [32]. The gEUDs of the PTV (assumption a = −10) and the sum of monitor units (MU) of each treatment plan were computed as well.

2.9. Statistical analysis

Patient data were coded in Excel and analyzed in SPSS version 26. Normality assumption of continuous variables was tested with the Kolmogorov–Smirnov and Shapiro–Wilk-tests. Descriptive statistics such as mean and standard-deviation (SD) (brain volume, NTCPs, actual doses (gEUDs of organs at risk as well as PTVs)) median and interquartile range (IQR) for non-normally distributed continuous variables (GTV, GTV/brain-ratio) were computed. In addition, 95% confidence intervals (95%CI) for the true mean and true TCP increase were computed. Pearson's correlation was used to test for associations between

target and brain volumes and NTCP. Paired-sample t-tests were conducted to compare the NTCPs of organs at risk, the gEUDs of the PTV as well as the TCPs between the homogenous and heterogenous plans. Results of statistical analysis with p-values <5% (0.05) were interpreted as statistically significant.

3. Results

3.1. Patient and tumor characteristics

CT datasets of 25 dogs with meningeal tumors were used for treatment planning. Demographics, OAR and tumor volumes of all dogs are depicted in as raw data, deposited in the open repository Harvard Dataverse [link will be added in final version]. Data was normally distributed according to Kolmogorov–Smirnov and Shapiro–Wilk-tests, except for GTV, CTV, PTV, optic chiasm volume, GTV/brain-ratio, and TCP of both heterogeneous plans (Plan 2_het 1 and Plan 3_het 2).

The median target volumes were as follows: GTV was 2.4 cm^3 (IQR 2.3), CTV 5.2 cm^3 (IQR 3.4), and PTV 10.9 cm^3 (IQR 5.3). Mean brain volumes were 83.4 cm^3 (SD±16.7), reflecting typical variation according to breed and dog body weight. Mean brainstem volume was 7.2 cm^3 (SD±2.3) and median optic chiasma volume 0.08 cm^3 (IQR 0.06), respectively. The median ratio of the GTV/brain ratio (relative tumor volume, GTV_{brain}) was 3.1% (IQR 2.2).

3.2. Plan comparison

For planning optimization we used $gEUD_{(a=4)}$ = 30.13 Gy for brain, $gEUD_{(a=6.3)}$ = 33.35 Gy for brainstem, and $gEUD_{(a=4)}$ = 35.74 Gy for the optic chiasm (chosen to keep NTCP ≤5%).

The gEUDs of the PTV, the dose relevant for tumor control, was higher for all deliberately heterogeneous planned plans: there was a significant difference in the gEUDs from Plan 1_hom (mean 39.93 Gy, SD±0.19) to Plan 2_het 1 (with the same NTCP) (mean 42.96 Gy, SD±0.90) conditions; t(24) = −16.7, $p < 0.001$). As expected, the differences in gEUDs were even larger from the Plan 1_hom to the Plan 3_het 2 (with the 5% NTCP) (mean 46.00 Gy, SD±3.4) conditions; t(24) = −8.95, $p < 0.001$). But also the 2 deliberately heterogeneous planned variants differed significantly: Plan 2_het 1 (mean 42.96 Gy, SD±0.90) vs. Plan 3_het 2 (mean 46.00 Gy, SD±3.4) conditions; t(24) = −4.62, $p < 0.001$). Median TCP of Plan 1_hom, Plan 2_het 1, and Plan 3_het 2 was 0.45 (IQR 0.27), 0.93 (IQR 0.12), and 1 (IQR 0.15), respectively. Figs. 2 and 3 depict two examples of DVHs from homogenously and deliberately heterogeneously planned patients.

In 5 of the 8 patients that were actually treated with an organ risk above the later tolerated 5%, the gEUD in the Plan 3_het 2 decreased. These 5 patients had tumors in the brainstem and were actually treated with corresponding NTCPs between 9.04–16.05%. The 3 patients with NTCPs close to and just above 5% were easily to be escalated with the heterogenous planning method. The NTCP distribution is graphically displayed for the three plan variants and different organs at risk in Fig. 4.

In the homogenous plans reflecting the treated situation, mean and median TCPs (Plan 1_hom) were rather low, with 42% (SD±20; 95% CI: 34, 51) and 50% (IQR: 27), respectively, ranging from 5%–86%. Mean and median TCPs of the same-risk plans (Plan 2_het 1) were 89% (SD±12; 95%CI: 84, 94) and 93% (IQR: 12) respectively, ranging from 53%–100%. The TCPs of the same-risk versus the homogeneous plans were significantly higher (mean 47% (SD±16, 95%CI: 40, 53), conditions; t(24)=−14.39, $p < 0.001$. Mean and median TCPs of the fixed-risk plans (Plan 3_het 2) were 87% (SD±24; 95%CI: 77, 97) and 99% (IQR: 15) respectively, ranging from 8%–100%. Also the TCPs of the fixed-risk versus the homogeneous plans were significantly higher (mean 45% (SD±31, 95%CI: 32, 58), conditions; t(24)=−7.16, $p < 0.001$). When the TCPs of the same-risk and fixed-risk plans were compared, significance was lost: mean 2% (SD±23, 95%CI: 7, 12), conditions; t(24)=−0.45, p =0.656).

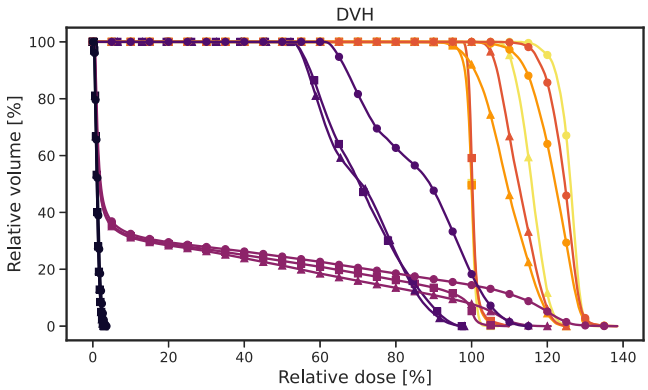

Fig. 2. DVH of patient with a meningioma in the cranial fossa: orange: PTV, red: CTV, yellow: GTV: The ■ -DVHs represent the homogenous plan (Plan 1_hom), ▲ -DVHs the heterogenous plan with the same NTCP (Plan 2_het 1), and the ● -DVH the heterogenous plan with the NTCP set at 5% (Plan 3_het 2) for brain (magenta) and optic chiasm (deep purple). The gEUD of the PTV increased to 107.4% in Plan 2_het 1, translating in a TCP increase of 69 percent points, and to 120.3% Plan 3_het 2, translating to a TCP increase of 77 percent points. (For interpretation of the references to color in this figure legend, the reader is referred to the web version of this article.)

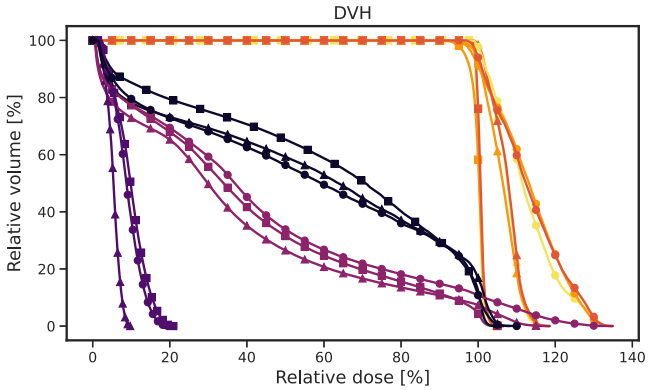

Fig. 3. DVH of patient with a meningioma in the caudal fossa (close to brainstem) and an initial NTCP of 5.7% in the brainstem: orange: PTV, red: CTV, yellow: GTV: GTV: The ■ -DVHs represent the homogenous plan (Plan 1_hom), ▲ -DVHs the heterogenous plan with the same NTCP (NTCP 5.7%, dark blue: brainstem = Plan 2_het 1). The gEUD of the PTV increased to 105.4% in Plan 2_het 1, translating in a TCP increase of 29 percent points. In spite of a lower NTCP of 5% in the ● -DVH (Plan 3_het 2), the gEUD of the PTV increased to 109.3% in Plan 3_het 2, translating also to a TCP increase of 29 percent points. (For interpretation of the references to color in this figure legend, the reader is referred to the web version of this article.)

Monitor units were lower in both heterogenous plan variants: Plan 1_hom (mean 880 MU, SD±105) and Plan 2_het 1 (with the same NTCP) (mean 743 MU, SD±86) conditions; t(24)=7.01, $p < 0.001$); and Plan 3_het 2 (with 5% NTCP) (mean 777 MU, SD±105) conditions; t(24)=3.65, $p = 0.001$). The monitor units between the two heterogenous plans did not differ significantly.

3.3. Model parameters

Fitting the population TCP including the volume variations with the detection rate limitation modified volume frequency distribution (Eq. (3)) to clinical data [33,40,41] yielded the parameter set α=0.37 Gy^{-1}, $\beta = 0.046$ Gy^{-2}, $a = 0.7$ yr^{-1} and $T_D = 4.5$ d with $\chi^2 = 0.285$. The 95% - confidence intervals determined by the bootstrapping method can be found in Table 1.

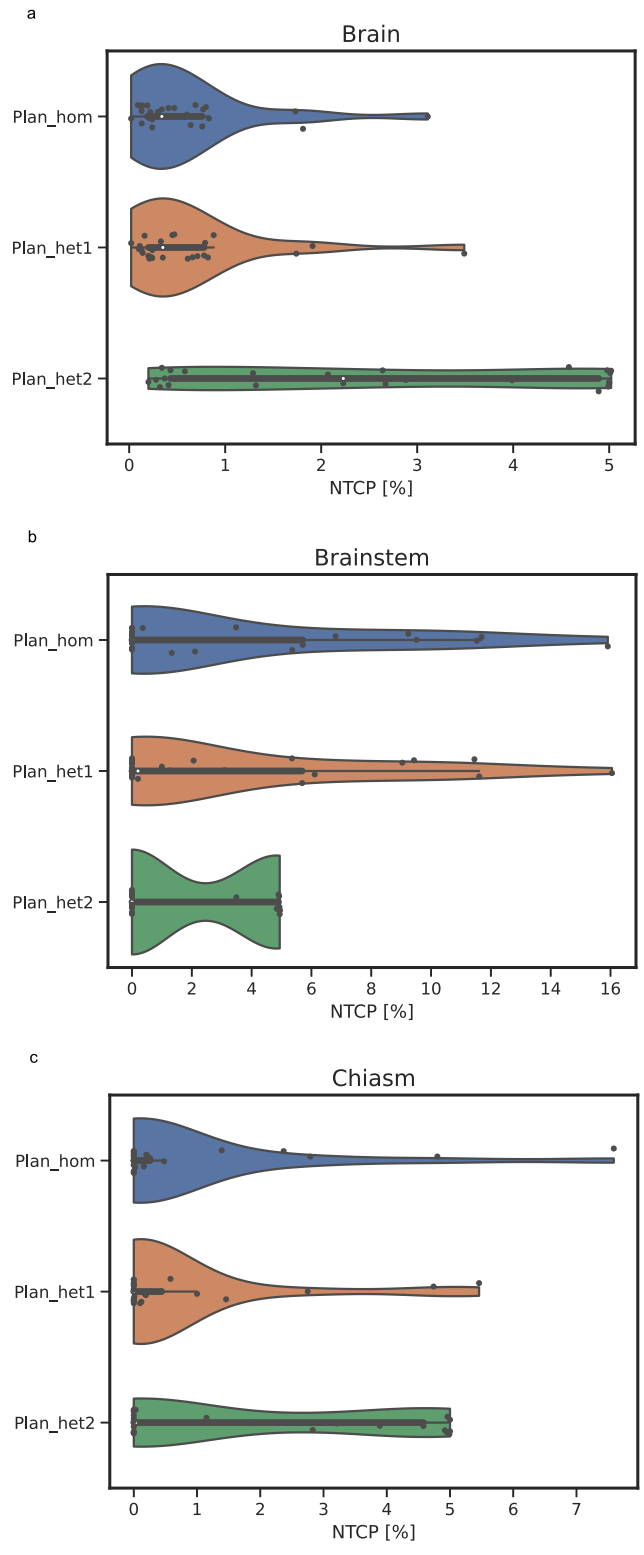

Fig. 4. NTCP distribution for the three plan variants and different organs at risk: (a) Brain, (b) Brainstem, (c) Chiasm.

3.4. TCP and TCP equivalent dose

In order to compare the homogeneous plans with the two different heterogeneous plans regarding TCP, in Fig. 5 the individual TCPs (Eq. (8)) for all plans and patients are plotted against their TCP equivalent doses. The error margins were also calculated for the TCP equivalent doses. As the errors $\sigma_{(D_{TCP_{equiv}})}$ were < 0.5 Gy for all points, we omitted them from the plot. Also plotted therein is the population TCP with its 68.2% confidence interval (corresponding to $\pm 1\sigma$). Further in Fig. 6 the $\Delta TCPs$ between the two heterogeneous plans and the homogeneous plan were plotted.

In Fig. 5, plotting the individual TCP values alongside the ensemble population TCP reveals a clustering around the ensemble values, indicating a good agreement. Further it was shown that heterogeneous plans in almost all cases lead to a higher TCP. On average the Plan2_het1 led to almost the same TCP increase as the Plan3_het2, however with a smaller increase in TCP equivalent (homogeneous) dose. In Fig. 6 it can be seen that Plan2_het1 (same-risk) leads to a smaller variation in TCP and TCP equivalent dose (tight cloud of red crosses), while for the Plan3_het2 (fixed-risk, green triangles) patients with tumor close to brainstem and optic chiasm are distributed at

Table 1
Model parameters and χ^2 obtained from fitting the population model (Eq. (3)) and their 95% confidence intervals obtained from bootstrapping.

	value	95% CI
α [Gy^{-1}]	0.37	[0.34–0.46]
a [yr^{-1}]	0.7	[0.16–1.47]
$T_D[d]$	4.5	[1.89–7.31]
χ^2	0.285	[0.05–0.38]

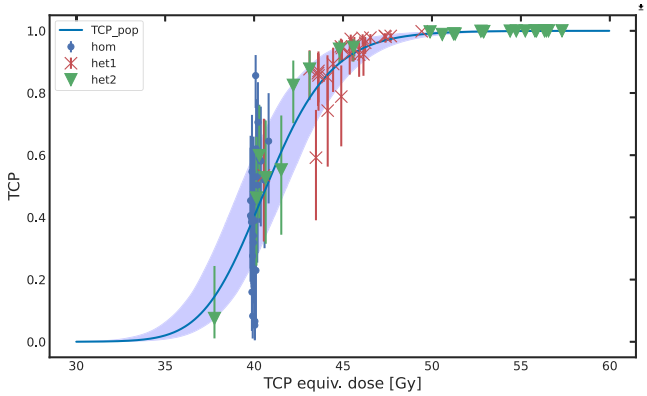

Fig. 5. Individual patient TCP values (as in Eq. (8)) resulting from Plan1_hom (blue dots), Plan2_het1 (red cross) and Plan3_het2 (green triangle) plotted versus corresponding TCP equivalent dose values (as in Eq. (15)). Also plotted is the population TCP with its 68.2% confidence interval (light blue). (For interpretation of the references to color in this figure legend, the reader is referred to the web version of this article.)

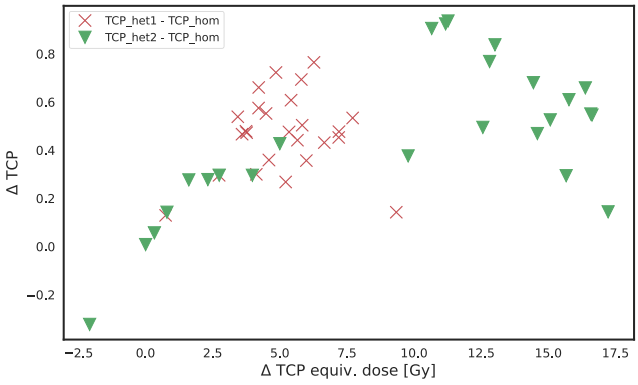

Fig. 6. Differences (Deltas) between the TCP of the respective heterogeneous plans and the homogeneous plan plotted as a function of the difference in the corresponding TCP equivalent dose: the tight cloud of red crosses represents same risk patients, while the green triangles represent patients with a fixed-risk, close to an OAR (left) or further away (right). (For interpretation of the references to color in this figure legend, the reader is referred to the web version of this article.)

Table 2
Obtained a parameters for the gEUD model; $\tilde{\mathbf{a}}$ are the median a values from the bootstrapping procedure.

Volume V [cm^3]	a	$\tilde{\mathbf{a}}$	68.8% CI	95% CI	# data pnts. N
<4	−24.8	−24.4	[−22.6, −27]	[−21.5, −33]	5
4–6	−24.6	−23.7	[−20, −29.1]	[−17.4, −43.5]	12
>6	−19.2	−19.3	[−16.1, −24.5]	[−13.9, −30.5]	8
all	−19.8	−19.5	[−16.8, −23.9]	[−15.4, −35.1]	25

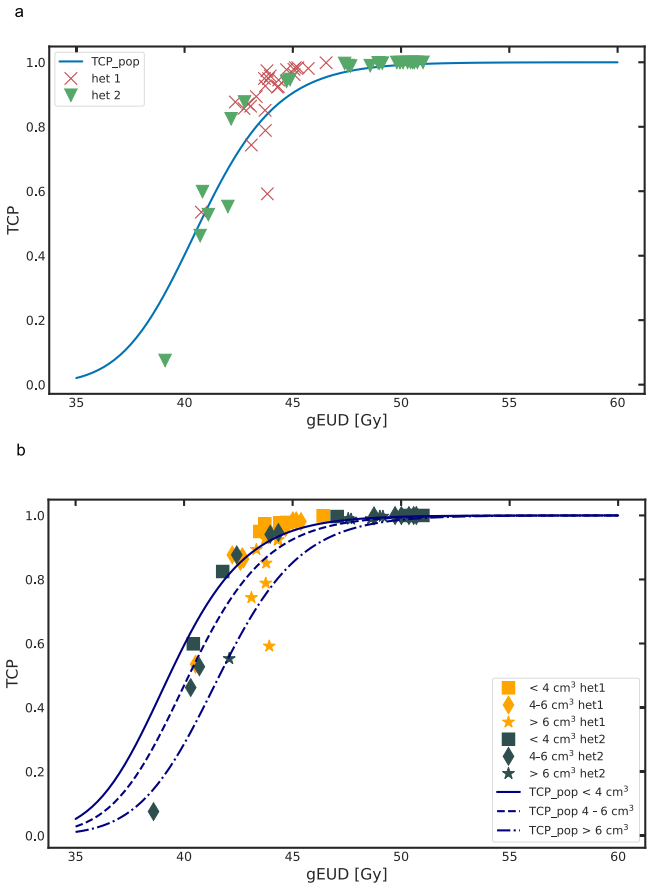

Fig. 7. TCP values plotted against the gEUDs computed with a_{opt}: (a) Single fit for all patients (b) Distinct fits for three different volume categories.

the lower end of TCP increase, while other patients can maximally benefit from heterogeneous, fixed-risk planning. For a single patient (1 out of 25) the Plan3_het2 even resulted in a TCP decrease. This was due to the very specific tumor location in that particular patient, which was very close to the brainstem. In the original homogenous plan (Plan1_hom) the NTCP was 15.91%. Limiting the NTCP in Plan3_het2 to 5% therefore led to a decrease in both TCP equivalent dose and TCP. This, however, might have prevented excessive brainstem toxicity in this patient.

3.5. Equivalent uniform dose

Table 2 holds the obtained a values from both the categorized and simultaneous fitting. It also contains the corresponding confidence intervals and median $\tilde{a}$ values. In Fig. 7a the TCP values for the Plan2_het1 and Plan3_het2 are plotted versus against their respective $gEUD$ values calculated with the a parameter obtained from simultaneous fitting to all data points (RT plans). The plotted cohort TCP was calculated for the mean tumor volume. In Fig. 7b the same was plotted but with categorization depending on the tumor volume.

4. Discussion

Prior work documented dose escalation using biology-based planning to increase the EUD without increasing expected risk of toxicity [10,50,51]. By setting a NTCP (or a gEUD for that matter) that is influenced by organ type, dose and volume, the treatment planner has to actively deprioritize the common goals of physical dose adherence. This leads to a somewhat uncomfortable situation: the comparison of two treatment plan options for the same patients do not have to fulfill an overlap in a steep PTV dose-volume histogram (DVH) anymore, but a plan's strength will be judged in the still less familiar term, the gEUD. In this study we tested the extent on how much the gEUD of most PTVs can be escalated by (a) using the same expected toxicities as the patient was treated and (b) by setting the expected toxicities at the chosen risk of 5%.

Our plan comparisons showed that the gEUD of the PTV and the TCP was higher for both of the heterogeneous plans (same-risk as well as fixed-toxicity), except for one patient with a tumor next to the brainstem. NTCP (for optic chiasm and the brain), on the other hand, was the same for the homogeneous (Plan 1_hom) and the same-risk heterogeneous plan (Plan 2_het) as expected, and highest in the fixed-risk heterogeneous plan (Plan 3_het).

Commonly used techniques such as stereotactic (body) radiation therapy (SRT/SBRT) or brachytherapy already allow dose heterogeneity within the tumor core [52,53]. In these techniques, heterogeneous (mostly hotter) areas in the tumors are tolerated up to about 1.3–1.4x the prescribed dose [54], but also underdosed volumes (0.5–0.7x the prescribed dose) can be found [55,56]. Such heterogeneous areas are usually caused by technical/physical reasons of beam application and not out of biological purpose. Furthermore, the stereotactic as well as brachytherapy approach has a limited range of indications. Our approach is different in that our dose escalation was actively forced and limited only by the organs at risk. Hereby, rather than satisfying physical constraints, the treatment plans were intended to produce a higher percentage of tumor control, while limited by the expected normal tissue damage. By using biological response models (gEUD/NTCP) during treatment planning, our herein proposed approach can be referred to as a biologically-based, in part risk-adaptive, personalized treatment planning approach. The EUD can be derived directly from an individual treatment plan dose-volume histogram and reflects the distribution of dose throughout a volume of interest. The TCP can then be derived from these dose calculation points by computing the expected number of surviving (tumor) clonogens, according to Poisson statistics [57]. Fogliata et al. [58] tested the performance of the gEUD objective in the Varian photon optimizer using different parameter values for a. They found that this tool can be useful in reducing organ at risk (OAR) dose for a range of parameter values [58]. As a current general draw-back there is a lack of consensus in parameter values of a. As a starting value for the gEUD optimization, however, some published values of the n parameter of the Lyman–Kutcher–Burman NTCP model could be considered (a = 1/n, and n values have been summarized) [28,59]. One danger of escalating dose within a tumor, is the potential risk of late toxicity, e.g. necrosis of normal structures such as vasculature and stroma within the PTV. As we intend to treat dog patients with sinonasal and brain tumors with such heterogeneously planned protocols, we limited our D2 at D2/130 (e.g. max 2% of PTV receives ≥ 52 Gy). Due to the moderately hypofractionated protocols in veterinary medicine, this was considered a safe approach for the dogs.

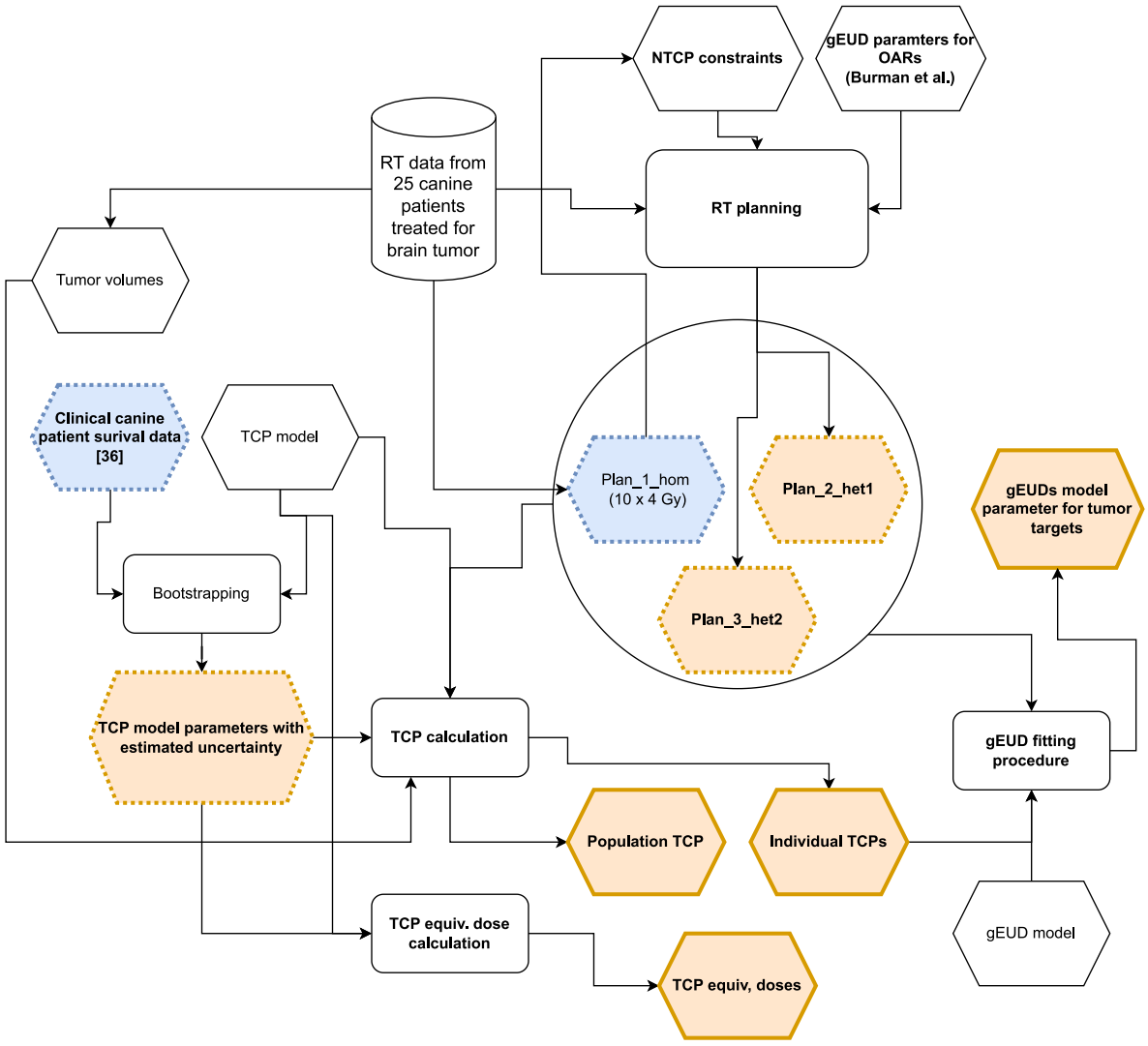

Fig. A.1. Overview of the methodology. The blue hexagons represent entities that have been created or assembled through our previous work. The orange hexagons represent entities which are results of this work. (For interpretation of the references to color in this figure legend, the reader is referred to the web version of this article.)

It was the goal, however, to increase the dose in as much of the tumor volume as possible, in order to increase TCP. In tumors containing high number of cells, little benefit of boosting by more than a 1.1 ratio was found by Tome et al. [10], unless a large part of the tumor volume (>90%) could be boosted. Furthermore, they observed that a maximum increase in TCP of about 16% could be expected. Smaller tumor and hot dose ratios of 1.5 given to 80% of the volume provided a larger gain of about 27% [10].

The herein calculated plans with the fixed-risk adherence (Plan 3_het) resulted in a 1.15 ratio of boost dose (gEUD). Our approach aims to increase the dose in as much volume as possible, which would be in line with the findings of Tome et al. [10]. When increasing dose by any means, radiosensitivity of the individual cell also remains important. In a clinical setting the radiosensitivity of individual cells is unknown and impossible to define. Nevertheless, a tumor cell can only be killed once. Any excessive dose to this cell must be considered “wasted”. In the concept of gEUD, however, this wasted dose will also increase the gEUD value but will not lead to increased TCP. This concept of wasted dose could also happen in a regular boost scenario.

Some limitations are worth noting: using human Quantitative Analyses of Normal Tissue Effects in the Clinic (QUANTEC) based constraints, a potential risk for animals might occur. It is not known in detail, if animals’ tissues react comparably. This limitation is known and an inherent problem in veterinary radiation oncology. However, the framework of interpolating human dose-volume constraints to animal tissues guided us through other theoretical calculations (brain tumors, anal sac adenocarcinoma) that were later tested in animals and safely so [31–33,60,61]. The human NTCP does not seem to underestimate toxicity in animals so far, and if it overestimates, we err on the safe side of the patient. For human patients, more data was gained from radiation protocols applied to brain, brainstem and optic nerve structures [36,37,62]. We herein assumed, that similar organs react in a similar manner in dogs, taken into account the different relative volume parameters. Validation of the use of gEUD organ targets in the clinical setting is achieved by forward planning with gEUD organ targets and then extracting NTCP data from the actual calculated plan.

5. Conclusion

Our study is a first step towards risk-adaptive radiation dose optimization. This strategy utilizes a biological objective function based on TCP and NTCP instead of an objective function based on physical dose constraints. A true risk-adaptive optimization, however, maximizes the objective function for different tumor risk regions while at the same time minimizing or limiting normal tissue complication probability [50]. The different tumor risk regions are often not known in detail

or could even change over the course of treatment, as seen in areas of fluctuating hypoxia or other microenvironmental conditions. However, the increases in TCP found herein with the use of organ-at-risk adaptive optimization warrant further investigation of this approach. Future work should therefore focus on clinical outcomes including follow-up designed to evaluate if TCP and complications are within the predicted range.

Funding

This work was supported by the Swiss National Science Foundation (SNSF), grant number: 320030-182490; PI: Carla Rohrer Bley

Declaration of competing interest

The authors declare that they have no known competing financial interests or personal relationships that could have appeared to influence the work reported in this paper.

Appendix

An overview of the methodology used in this study is given in Fig. A.1.

References

[1] Zelefsky MJ, Fuks Z, Hunt M, Lee HJ, Lombardi D, Ling CC, et al. High dose radiation delivered by intensity modulated conformal radiotherapy improves the outcome of localized prostate cancer. J Urol 2001;166(3):876–81,.

[2] Chargari C, Magne N, Guy J-B, Rancoule C, Levy A, Goodman KA, et al. Optimize and refine therapeutic index in radiation therapy: Overview of a century. Cancer Treatment Rev 2016;45:58–67. http://dx.doi.org/10.1016/j.ctrv.2016.03.001,.

[3] Cho KH, Kim J-Y, Lee SH, Yoo H, Shin SH, Moon SH, et al. Simultaneous integrated boost intensity-modulated radiotherapy in patients with high-grade gliomas.. Int J Radiat Oncol Biol Phys 2010;78(2):390–7. http://dx.doi.org/10.1016/j.ijrobp.2009.08.029,.

[4] Orlandi E, Palazzi M, Pignoli E, Fallai C, Giostra A, Olmi P. Radiobiological basis and clinical results of the simultaneous integrated boost (SIB) in intensity modulated radiotherapy (IMRT) for head and neck cancer: A review. Critical Rev Oncol Hematol 2010;73(2):111–25. http://dx.doi.org/10.1016/j.critrevonc.2009.03.003,.

[5] Okunieff P, Morgan D, Niemierko A, Suit HD. Radiation dose-response of human tumors. Int J Radiat Oncol Biol Phys 1995;32(4):1227–37. http://dx.doi.org/10.1016/0360-3016(94)00475-Z.

[6] Grégoire V, Haustermans K, Geets X, Roels S, Lonneux M. PET-based treatment planning in radiotherapy: a new standard? J Nuclear Med Official Publ Soc Nuclear Med 2007;48 Suppl 1:68S–77S,.

[7] Shi X, Meng X, Sun X, Xing L, Yu J. PET/CT imaging-guided dose painting in radiation therapy. Cancer Lett 2014;355(2):169–75. http://dx.doi.org/10.1016/j.canlet.2014.07.042,.

[8] Thorwarth D, Geets X, Paiusco M. Physical radiotherapy treatment planning based on functional PET/CT data.. Radiother Oncol J Eur Soc Therapeut Radiol Oncol 2010;96(3):317–24. http://dx.doi.org/10.1016/j.radonc.2010.07.012,.

[9] Bentzen SM, Gregoire V. Molecular imaging-based dose painting: a novel paradigm for radiation therapy prescription.. Seminars Radiat Oncol 2011;21(2):101–10. http://dx.doi.org/10.1016/j.semradonc.2010.10.001,.

[10] Tome WA, Fowler JF. Selective boosting of tumor subvolumes. Int J Radiat Oncol Biol Phys 2000;48(2):593–9. http://dx.doi.org/10.1016/s0360-3016(00)00666-0,.

[11] Barnett GC, West CML, Dunning AM, Elliott RM, Coles CE, Pharoah PDP, et al. Normal tissue reactions to radiotherapy: towards tailoring treatment dose by genotype. Nat Rev Cancer 2009;9(2):134–42. http://dx.doi.org/10.1038/nrc2587,.

[12] Moran JM, Elshaikh MA, Lawrence TS. Radiotherapy: what can be achieved by technical improvements in dose delivery? Lancet Oncol 2005;6(1):51–8. http://dx.doi.org/10.1016/S1470-2045(04)01713-9,.

[13] Tommasino F, Nahum A, Cella L. Increasing the power of tumour control and normal tissue complication probability modelling in radiotherapy: recent trends and current issues. Transl Cancer Res 2017;6(Suppl 5). URL https://tcr.amegroups.org/article/view/14116.

[14] Emami B, Lyman J, Brown A, Coia L, Goitein M, Munzenrider JE, et al. Tolerance of normal tissue to therapeutic irradiation. Int J Radiat Oncol Biol Phys 1991;21(1):109–22. http://dx.doi.org/10.1016/0360-3016(91)90171-y,.

[15] Constine LS, Milano MT, Friedman D, Morris M, Williams JP, Rubin P, et al. Late effects of cancer treatment on normal tissues. In: Halperin EC, Perez CA, Brady LW, editors. Principles and practice of radiation oncology. Lippincott Williams & Wilkins; 2008, p. 320–55.

[16] Ten Haken RK, Martel MK, Kessler ML, Hazuka MB, Lawrence TS, Robertson JM, et al. Use of veff and iso-NTCP in the implementation of dose escalation protocols.. Int J Radiat Oncol Biol Phys 1993;27(3):689–95. http://dx.doi.org/10.1016/0360-3016(93)90398-f,.

[17] Nahum AE, Uzan J. (Radio)biological optimization of external-beam radiotherapy.. Comput Math Methods Med 2012;2012:329214. http://dx.doi.org/10.1155/2012/329214,.

[18] Sanchez-Nieto B, Nahum AE, Dearnaley DP. Individualization of dose prescription based on normal-tissue dose-volume and radiosensitivity data.. Int J Radiat Oncol Biol Phys 2001;49(2):487–99. http://dx.doi.org/10.1016/s0360-3016(00)01508-x,.

[19] Yorke E. Biological indices for evaluation and optimization of IMRT. In: Palta JTM, ed. teletherapy: present and future. American Association of Physicists in Medicine, College Park; 2003.

[20] Bentzen SM, Tucker SL. Quantifying the position and steepness of radiation dose-response curves. Int J Radiat Biol 1997;71(5):531–42. http://dx.doi.org/10.1080/095530097143860,.

[21] Goitein M, Schultheiss TE. Strategies for treating possible tumor extension: some theoretical considerations. Int J Radiat Oncol Biol Phys 1985;11(8):1519–28. http://dx.doi.org/10.1016/0360-3016(85)90341-4,.

[22] Munro TR, Gilbert CW. The relation between tumour lethal doses and the radiosensitivity of tumour cells. Br J Radiol 1961;34:246–51. http://dx.doi.org/10.1259/0007-1285-34-400-246,.

[23] Goitein M, Niemierko A. Intensity modulated therapy and inhomogeneous dose to the tumor: a note of caution. Int J Radiat Oncol Biol Phys 1996;36(2):519–22. http://dx.doi.org/10.1016/s0360-3016(96)00348-3,.

[24] Lyman JT. Complication probability as assessed from dose-volume histograms.. Radiat Res Suppl 1985;8:S13–9,.

[25] Wheldon TE, Deehan C, Wheldon EG, Barrett A. The linear-quadratic transformation of dose-volume histograms in fractionated radiotherapy. Radiother Oncol J Eur Soc Therapeut Radiol Oncol 1998;46(3):285–95. http://dx.doi.org/10.1016/s0167-8140(97)00162-x,.

[26] Goitein M. Radiation oncology: a physicist's-eye view. Biological and medical physics, biomedical engineering, Springer New York; 2007, URL https://books.google.ch/books?id=C8z8dL5eBnQC.

[27] Niemierko A, Goitein M. Implementation of a model for estimating tumor control probability for an inhomogeneously irradiated tumor.. Radiother Oncol J Eur Soc Therapeut Radiol Oncol 1993;29(2):140–7. http://dx.doi.org/10.1016/0167-8140(93)90239-5,.

[28] Allen Li X, Alber M, Deasy JO, Jackson A, Ken Jee K-W, Marks LB, et al. The use and QA of biologically related models for treatment planning: short report of the TG-166 of the therapy physics committee of the aapm.. Med Phys 2012;39(3):1386–409. http://dx.doi.org/10.1118/1.3685447,.

[29] Widesott L, Strigari L, Pressello MC, Benassi M, Landoni V. Role of the parameters involved in the plan optimization based on the generalized equivalent uniform dose and radiobiological implications.. Phys Med Biol 2008;53(6):1665–75. http://dx.doi.org/10.1088/0031-9155/53/6/011,.

[30] Wu Q, Mohan R, Niemierko A, Schmidt-Ullrich R. Optimization of intensity-modulated radiotherapy plans based on the equivalent uniform dose.. Int J Rad Oncol Biol Phys 2002;52(1):224–35. http://dx.doi.org/10.1016/s0360-3016(01)02585-8,.

[31] Meier V, Besserer J, Rohrer Bley C. Using biologically based objectives to optimize boost intensity-modulated radiation therapy planning for brainstem tumors in dogs.. Vet Radiol Ultrasound J Am College Veterinary Radiol Int Veterinary Radiol Assoc 2020;61(1):77–84. http://dx.doi.org/10.1111/vru.12815,.

[32] Rohrer Bley C, Meier V, Schwarz P, Roos M, Besserer J. A complication probability planning study to predict the safety of a new protocol for intracranial tumour radiotherapy in dogs.. Vet Comp Oncol 2017;15(4):1295–308. http://dx.doi.org/10.1111/vco.12265,.

[33] Schwarz P, Meier V, Soukup A, Drees R, Besserer J, Beckmann K, et al. Comparative evaluation of a novel, moderately hypofractionated radiation protocol in 56 dogs with symptomatic intracranial neoplasia. J Veterinary Int Med 2018;32(6):2013–20. http://dx.doi.org/10.1111/jvim.15324.

[34] Vol I. Prescribing, recording, and reporting photon-beam intensity-modulated radiation therapy (IMRT): contents. J ICRU 2010;10.

[35] Rohrer Bley C, Meier VS, Besserer J, Schneider U. Intensity-modulated radiation therapy dose prescription and reporting: Sum and substance of the international commission on radiation units and measurements report 83 for veterinary medicine.. Vet Radiol Ultrasound J Am College Veterinary Radiol Int Veterinary Radiol Assoc 2019;60(3):255–64. http://dx.doi.org/10.1111/vru.12722,.

[36] Mayo C, Martel MK, Marks LB, Flickinger J, Nam J, Kirkpatrick J. Radiation dose-volume effects of optic nerves and chiasm.. Int J Radiat Oncol Biol Phys 2010;76(3 Suppl):S28–35. http://dx.doi.org/10.1016/j.ijrobp.2009.07.1753,.

[37] Mayo C, Yorke E, Merchant TE. Radiation associated brainstem injury.. Int J Radiat Oncol Biol Phys 2010;76(3 Suppl):S36–41. http://dx.doi.org/10.1016/j.ijrobp.2009.08.078,.

[38] Burman C, Kutcher GJ, Emami B, Goitein M. Fitting of normal tissue tolerance data to an analytic function.. Int J Radiat Oncol Biol Phys 1991;21(1):123–35. http://dx.doi.org/10.1016/0360-3016(91)90172-z,.

[39] Radonic S, Besserer J, Meier V, Bley CR, Schneider U. A novel analytical population tumor control probability model includes cell density and volume variations: Application to canine brain tumor. Int J Radiat Oncol Biol Phys 2021;110(5):1530–7. http://dx.doi.org/10.1016/j.ijrobp.2021.03.021.

[40] Bley CR, Sumova A, Roos M, Kaser-Hotz B. Irradiation of brain tumors in dogs with neurologic disease. J Veterinary Int Med 2005;19(6):849–54. http://dx.doi.org/10.1892/0891-6640(2005)19[849:IOBTID]2.0.CO;2.

[41] Keyerleber MA, Mcentee MC, Farrelly J, Thompson MS, Scrivani PV, Dewey CW. Three-dimensional conformal radiation therapy alone or in combination with surgery for treatment of canine intracranial meningiomas. Veterinary Comparat Oncol 2015;13(4):385–97. http://dx.doi.org/10.1111/vco.12054.

[42] Schneider U, Besserer J. Tumour volume distribution can yield information on tumour growth and tumour control. Z Med Phys 2021. http://dx.doi.org/10.1016/j.zemedi.2021.04.002, URL https://www.sciencedirect.com/science/article/pii/S0939388921000532.

[43] Dale RG. Radiobiological assessment of permanent implants using tumour repopulation factors in the linear-quadratic model. Br J Radiol 1989;62(735):241–4. http://dx.doi.org/10.1259/0007-1285-62-735-241, PMID: 2702381.

[44] Li XA, Wang JZ, Stewart RD, DiBiase SJ. Dose escalation in permanent brachytherapy for prostate cancer: Dosimetric and biological considerations. Phys Med Biol 2003;48(17):2753–65. http://dx.doi.org/10.1088/0031-9155/48/17/302.

[45] Efron B. Bootstrap methods: Another look at the jackknife. Ann Statist 1979;7(1):1–26. http://dx.doi.org/10.1214/aos/1176344552.

[46] Nahum AE, Tait DM. Maximizing local control by customized dose prescription for pelvic tumours. In: Breit A, Heuck A, Lukas P, Kneschaurek P, Mayr M, editors. Tumor response monitoring and treatment planning. Berlin, Heidelberg: Springer Berlin Heidelberg; 1992, p. 425–31.

[47] Webb S, Nahum AE. A model for calculating tumour control probability in radiotherapy including the effects of inhomogeneous distributions of dose and clonogenic cell density. Phys Med Biol 1993;38(6):653–66. http://dx.doi.org/10.1088/0031-9155/38/6/001.

[48] Fowler JF. The linear-quadratic formula and progress in fractionated radiotherapy. Br J Radiol 1989;62(740):679–94. http://dx.doi.org/10.1259/0007-1285-62-740-679, PMID: 2670032.

[49] Qi XS, Schultz CJ, Li XA. An estimation of radiobiologic parameters from clinical outcomes for radiation treatment planning of brain tumor. Int J Radiat Oncol Biol Phys 2006;64(5):1570–80. http://dx.doi.org/10.1016/j.ijrobp.2005.12.022.

[50] Kim Y, Tomé WA. Risk-adaptive optimization: selective boosting of high-risk tumor subvolumes. Int J Radiat Oncol Biol Phys 2006;66(5):1528–42. http://dx.doi.org/10.1016/j.ijrobp.2006.08.032,.

[51] Kim Y, Tome WA. Is it beneficial to selectively boost high-risk tumor subvolumes? A comparison of selectively boosting high-risk tumor subvolumes versus homogeneous dose escalation of the entire tumor based on equivalent eud plans.. Acta Oncol (Stockholm, Sweden) 2008;47(5):906–16. http://dx.doi.org/10.1080/02841860701843050,.

[52] Lo SS, Fakiris AJ, Chang EL, Mayr NA, Wang JZ, Papiez L, et al. Stereotactic body radiation therapy: a novel treatment modality.. Nat Rev Clin Oncol 2010;7(1):44–54. http://dx.doi.org/10.1038/nrclinonc.2009.188,.

[53] Taylor ML, Kron T, Franich RD. A contemporary review of stereotactic radiotherapy: inherent dosimetric complexities and the potential for detriment.. Acta Oncol (Stockholm, Sweden) 2011;50(4):483–508. http://dx.doi.org/10.3109/0284186X.2010.551665,.

[54] Giglioli FR, Clemente S, Esposito M, Fiandra C, Marino C, Russo S, et al. Frontiers in planning optimization for lung sbrt.. Phys Med Int J Devot Appl Phys Med Biol Official J Italian Assoc Biomed Phys (AIFB) 2017;44:163–70. http://dx.doi.org/10.1016/j.ejmp.2017.05.064,.

[55] D'Souza WD, Thames HD, Kuban DA. Dose-volume conundrum for response of prostate cancer to brachytherapy: summary dosimetric measures and their relationship to tumor control probability.. Int J Radiat Oncol Biol Phys 2004;58(5):1540–8. http://dx.doi.org/10.1016/j.ijrobp.2003.09.016,.

[56] Roosen J, Klaassen NJM, Westlund Gotby LEL, Overduin CG, Verheij M, Konijnenberg MW, et al. To 1000 gy and back again: a systematic review on dose-response evaluation in selective internal radiation therapy for primary and secondary liver cancer.. Eur J Nuclear Med Molecular Imag 2021;48(12):3776–90. http://dx.doi.org/10.1007/s00259-021-05340-0,.

[57] Niemierko A. Reporting and analyzing dose distributions: a concept of equivalent uniform dose. Med Phys 1997;24(1):103–10. http://dx.doi.org/10.1118/1.598063,.

[58] Fogliata A, Thompson S, Stravato A, Tomatis S, Scorsetti M, Cozzi L. On the gEUD biological optimization objective for organs at risk in photon optimizer of eclipse treatment planning system.. J Applied Clinical Med Phys 2018;19(1):106–14. http://dx.doi.org/10.1002/acm2.12224,.

[59] Wu Q, Djajaputra D, Wu Y, Zhou J, Liu HH, Mohan R. Intensity-modulated radiotherapy optimization with gEUD-guided dose-volume objectives.. Phys Med Biol 2003;48(3):279–91. http://dx.doi.org/10.1088/0031-9155/48/3/301,.

[60] Soukup A, Meier V, Pot S, Voelter K, Rohrer Bley C. A prospective pilot study on early toxicity from a simultaneously integrated boost technique for canine sinonasal tumours using image-guided intensity-modulated radiation therapy. Veterinary Compar Oncol 2018;16(4):441–9. http://dx.doi.org/10.1111/vco.12399,.

[61] Körner M, Staudinger C, Meier V, Rohrer Bley C. Retrospective assessment of radiation toxicity from a definitive-intent, moderately hypofractionated image-guided intensity-modulated protocol for anal sac adenocarcinoma in dogs. Veterinary Compar Oncol 2022;20(1):8–19. http://dx.doi.org/10.1111/vco.12701, arXiv:https://onlinelibrary.wiley.com/doi/pdf/10.1111/vco.12701.

[62] Lawrence YR, Li XA, el Naqa I, Hahn CA, Marks LB, Merchant TE, et al. Radiation dose-volume effects in the brain.. Int J Radiat Oncol Biol Phys 2010;76(3 Suppl). http://dx.doi.org/10.1016/j.ijrobp.2009.02.091, S20–7.